Molecular BioSystems

Accepted Manuscript

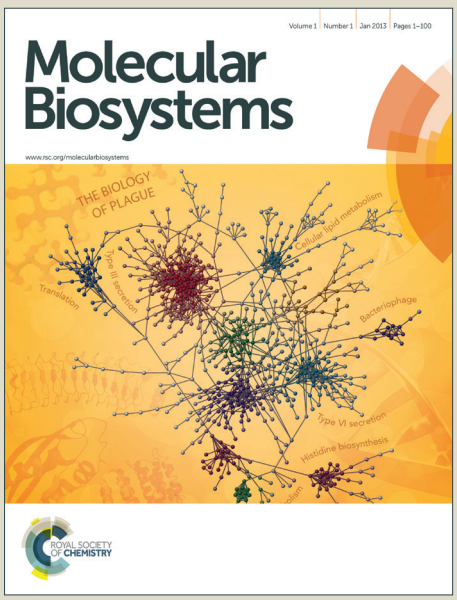

ROYAL SOCIETY OF CHEMISTRY

www.rsc.org/molecularbiosystems

The plasma metabolic profiling of chronic acephate exposure in rat via ultra-performance liquid chromatography-mass spectrometry based metabonomic method

Yurong Hou[a1], Can Cao[a1], Wei Bao[a], Shuang Yang[a], Haidan Shi[a], Dongfang Hao[a], Xiujuan Zhao[a*], and Yonghui Wu[a*]

[a] Public Health College, Harbin Medical Unviersity, Harbin, Heilongjiang, China.

[1] They contributed equally to this work and should be considered as co-first authors.

[*] To whom correspondence should be addressed at Harbin Medical University, 194 Xuefu Road, NangangDistrict, P.R.China, 150081.

Tel: +8645187502731, Fax: +8645187502885.

E-mail: xiujuan_zhao@sina.com (Xiujuan Zhao) Or wuyonghui777@163.com (Yonghui Wu).

Abstract

This study aimed to investigate the toxic effect of long-term, low-dose acephate administration on rats by ultra-performance liquid chromatography-mass spectrometry. A total of 120 male Wistar rats were randomly assigned to different groups: control; low-dose acephate (0.5 mg/kg·bw); middle-dose acephate (1.5 mg/kg·bw); and high-dose acephate (4.5 mg/kg·bw). The rats continuously received acephate via drinking water for 24 weeks. Rat plasma samples were collected at different time points to measure metabonomic profiles. Liver tissues were subjected to histopathological examination. Results showed that 10 metabolites in the plasma were significantly changed in the treated groups compared with those in the control group ($P < 0.05$ or $P < 0.01$). Exposure to acephate resulted in increased lysoPC (15:0), lysoPC (16:0), lysoPC (O-18:0), lysoPC (18:1(9Z)), lysoPC (18:0), lysoPC (20:4(5Z, 8Z, 11Z, 14Z)), arachidonic acid, and 12-HETE as well as decreased tryptophan and indoleacrylic acid in rat plasma. Moreover, the contents of high-density lipoprotein, low-density lipoprotein, triglyceride, total cholesterol, free fatty acids, and malondialdehyde, as well as the activities of superoxide dismutase and phospholipaseA2 in the serum, were significantly changed in middle- and high-dose groups compared with those in the control group ($P < 0.05$ or $P < 0.01$). Histopathological examination results revealed that exposure to acephate may induce vacuolar degeneration in the liver cell cytoplasm, fat degeneration, and liver cell necrosis. These results indicated that exposure to acephate disrupted metabolism of

lipids and amino acids, induced oxidative stress, caused neurotoxicity, and resulted in liver dysfunction.

Key words: Acephate; Metabonomics; Toxicity; Rat; Plasma; No observed adverse effect level.

1. Introduction

Organophosphorus (OP) pesticides are widely used in China because of their highly effective insecticidal activities, low cost, and wide varieties. Acephate (*O*, *S*-dimethyl-*N*-acetyl phosphoramidothioate) is an organophosphorus insecticide that is widely applied to protect vegetables and fruits from moths and aphids.[1-4] However, the extensive use of acephate has increased human exposure via different sources, including residues in food and water, applications to public spaces, and occupational means.[5, 6] Acephate is present at low levels but persistent for long periods of time. Therefore, adverse effects of acephate exposure on human health should be studied further.[7]

Acephate is known as an inhibitor of acetylcholinesterase activity.[8] Toxicological studies on acephate have focused on acute toxicity, short-term and long-term toxicities, genotoxicity, reproductive toxicity, and neurotoxicity.[9] Specific in vivo studies on acephate-related toxicities have also been conducted.[10-15] Studies have revealed that acephate may induce CYP superfamily perturbation in different tissues of CD1 mice[10]

and caused genotoxicity in the leukocytes of mice.[11] Previous studies also reported that acephate is a clastogenic and cytotoxic agent that causes DNA damage at high concentrations in human lymphocyte cultures.[12] Moreover, other studies have indicated that acephate can affect antioxidant defense systems.[13-15] Although the toxicity of acephate has been well studied, [10-15] very few toxicological studies concerning systemic metabolic responses to chronic low-dose exposure to acephate have been reported.[7] Therefore, a new research method should be developed to investigate the toxic effects of low-dose and long-term exposure to acephate.

Metabonomics is an important component of systems biology and defined as "the quantitative measurement of the dynamic multiparametric metabolic response of living systems to pathophysiological stimuli or genetic modification".[16] Metabonomics focuses on the analysis of low-molecular weight metabolites in biofluids, such as plasma, urine, and saliva, or tissues, which represent the functional phenotype in a system under a specified set of conditions emphasizing the whole system rather than individual parts. As a global metabolic profiling framework, metabonomics utilizes high-resolution analytics, together with chemometric statistical tools, to derive an integrated map of endogenous and xenobiotic metabolites. Metabonomics has shown a great potential to providing further insights into disease process, biomarker identification, and toxicological mechanisms.[17-19] Dudka *et al*.[20] assessed the alterations of metabolic profiles of serum in workers who were occupationally exposed to a mixture of heavy metals; this assessment shows that metabonomics is a very reliable technology to study the biochemical effects induced

by mixtures of heavy metals. In view of the characteristic advantages, metabonomics has been extensively investigated in the field of toxicology.[21-23] Although the metabonomics has been widely used in the field of toxicology, the mechanisms of toxicity of chronic exposure to acephate have not been completely elucidated based on this technology, except for our previous published article which studied the toxicity induced by acephate in urine.[7]

No observed adverse effect level (NOAEL) is defined as "the highest level of continual exposure to a chemical that causes no significant adverse effect on the morphology, biochemistry, functional capacity, growth, development, or life span of target species as determined by traditional toxicology," which was obtained using traditional toxicological methods. Considering that metabonomics shows several advantages, including efficiency, rapid separation, and high sensitivity, we performed ultra-performance liquid chromatography-mass spectrometry (UPLC-MS) in this study to investigate if chronic exposure to acephate at NOAEL could induce toxicity on rats at body metabolism level; this study was also conducted to identify potential exposure biomarkers and toxic mechanism of acephate.

2. Materials and methods

2.1 Chemicals

Acephate (purity > 95%) was purchased from Nantong Weilike Chemical Co. Ltd. (Nantong, China). HPLC-grade methanol and acetonitrile were supplied by Dikma Science and Technology, Co. Ltd. (Toronto, Ontario, Canada). Distilled water was filtered using a Milli-Q Ultrapure water system (Millipore, Billerica, USA). Leucine

enkephalin was obtained from Sigma-Aldrich (St Louis, Missouri, USA). High-density lipoprotein (HDL), low-density lipoprotein (LDL), triglyceride (TG), total cholesterol (TCHO) were purchased from BioSino Bio-technology and Science Inc. (Beijing, China). Diagnostic kits for free fatty acids (FFA), malondialdehyde (MDA), superoxide dismutase (SOD) and enzyme-linked immunosorbent assay (ELISA) kits for phospholipaseA2 (PLA2) were obtained from Nanjing Jiancheng Bioengineering Institute (Nanjing, China).

2.2 Animal treatment

A total of 120 male Wistar rats (6 weeks old, weighing approximately 180-220 g) were supplied by Vital River Laboratory Animal Technology Co. Ltd. (Beijing, China). Rats were housed individually in wire cages under controlled humidity (50-60%) and temperature (22±2°C) with a light/dark cycle of 12h. Throughout the study period, all rats had free access to AIN-93M diets and drinking water and allowed at least 1 week to adapt to laboratory environment before experiments. Animal handling were carried out in accordance with Chinese legislation on the use and care of laboratory animals and with the guidelines established by the Institute of Zoology, Animal and Medical Ethics Committee of Harbin Medical University.

After acclimatization, rats were randomly divided into four groups (n=30, each group was further randomly divided into six subgroups): low-dose group (0.5 mg/kg·bw, NOAEL), middle-dose group (1.5 mg/kg·bw, three times the NOAEL), high-dose group (4.5 mg/kg·bw, nine times the NOAEL), and control group. According to the dose of each group, acephate was given to rats by drinking water ad

libitum, whereas the control rats were recieved an equivalent volume of drinking water. Daily water volume given to each rat was its average amount of water consumption last week plus 5ml drinking water. Water consumption increased from 24 ml to 40 ml in the first 5 weeks after dosing and maintained at about 40 ml until the end of the treatment. Water consumption at every week showed no significantly changes in the treated groups compared with the time-matched control group ($P > 0.05$). All animals received the treatment for a continually 24 weeks.

2.3 Sample collection

Each subgroup (n=5) was randomly selected from each dose group at 4, 8, 12, 16, 20 and 24 weeks after treatment, and anesthetized using pentobarbital, abdominal aorta blood samples were collected. The blood samples were divided into two aliquots, serum was obtained from one aliquot by centrifugation at 3000 rpm for 15min after the blood samples clotted, then analyzed using a Hitachi 7100 automated biochemical analyzer (Hitachi Co. Japan) to test for HDL, LDL, TG and TCHO. The other blood samples were collected using 5ml anticoagulant tubes. Tubes were shaken to mix the anticoagulant with the blood, then centrifuge at 3000rpm for 15min. The obtained plasma was transferred into Eppendorf tubes and stored at -80°C for metabonomics analysis.

2.4 Histopathology

The liver of each rat was excised for histopathological analysis immediately after blood collection. Liver samples were fixed in 10% formalin. The samples were dehydrated by standard procedures and embedded in paraffin blocks. Sections about

4μm thick were cut, stained with haematoxylin eosin, and examined by light microscope.

2.5 Sample preparation

Before UPLC-MS analysis, the protein of plasma should precipitated by adding 450 μL methanol to 150 μL of plasma in a tube followed by vortex shaking for 2 min at room temperature and centrifuged at 12000 rpm for 10 min at 4°C to remove any precipitate. The supernatant was transferred to a new tube, drying by a Bath Nitrogen Blow Instrument (TTL-DCI, Beijing, China), reconstituted in a 600 μL acetonitrile and water mixture (2:1, V/V). The mixture was vortexed for 2 min, and then centrifuged at 12000 rpm for 10 min. The supernatant was set aside until use for the UPLC-MS analysis.

2.6 Chromatography

Chromatographic separation was achieved on a UPLC-BEH C18 column (100×2.1mm, i.d. 1.7 μm, 130 Å, Waters Corporation, Milford, Massachusetts, USA) using a Waters ACQUITY UPLC System (Waters Corporation). A 2μL aliquot of the sample was injected into the columns. The temperature of the column was kept constant at 35°C. The mobile phase consisted of water with 0.1% formic acid (A) and acetonitrile (B). The flow rate was 0.35mL/min and the gradient duration was 16 min. The gradient profile used for the separation was using a linear gradient of 2% B for 0.5 min, 2-20% B for 0.5-1.5 min, 20-70% B for 1.5-6 min, 70-98% B for 6-10 min, 98% B for 10-12 min, 98-70% B for 12-14 min, 70-2% B for 14-16 min. A needle wash cycle was performed after every sample injection to remove sample remnants

and to prepare the equipment for the next injection. In addition, the eluent was directly transferred to the MS in a split mode.

2.7 Mass spectrometry

The mass spectrometric datas were collected using Waters Micromass Quatropde-Time of Flight (Q-TOF) micro Mass Spectrometer (Manchester, UK) equipped with electrospray ionization (ESI) which has a full scan mode from m/z 50 to 1000 and 0 to 16 min in both positive and negative modes. Nitrogen served as both the desolvation gas and cone gas with the flow rate of 650 and 50 L/h, respectively. 300°C and 50 °C are used as the temperatures of desolvation and source, respectively. The capillary voltage was set to 3.0 kV in the positive ion mode and 2.8 kV in the negative ion mode, and the cone voltage was set to 35 V. In order to ensure the accuracy and reproducibility of all analyses, a lock mass of leucine enkephalin was used via a lock spray interface at a flow rate of 10μL/min for monitoring in the positive ($[M+H]^+$=556.2771) and negative ion modes ($[M-H]^-$=554.2615). The lock spray frequency was set at 0.48s, and the lock mass data were averaged over 10 scans for correction.

2.8 Metabolite identification

The data matrix including peak numbers (retention time-*m*/*z* pairs), sample names and ion intensities were introduced into the EZinfo software for multivariate statistical analysis via principal component analysis (PCA) and partial least quares-discriminant analysis (PLS-DA) which were used to obtain the biomarkers. With regard to the choice of biomarkers, variables were selected based on a threshold of Variable

Importance in Projection (VIP) values and the loading plots. The metabolites with VIP value >1.0 and those are dominant in the loading plots would be considered important in discriminating between different groups. The metabolite was searched by probable elementary composition and properties in-house or using the online ChemSpider database to narrow down range of identification. Metabolites were identified by comparing the retention times and MS spectra in standard library. To support the metabolite identification, the following databases have been used: the Human Metabolome Database, Scripps Center for Metabolomics, MassBank, and LIPID MAPS.

2.9 Data analysis

Statistical analysis was performed by covariance (ANCOVA) and one-way ANOVA using SPSS (version 13.0; Beijing Stats Data Mining Co. Ltd., China) and $P < 0.05$ was considered statistically significant.

The UPLS-MS data files were processed by Micromass Markerlynx Application Version 4.1 (Waters, Milford, MA), which allowed data deconvolution, alignment, and reduction to yield a table of mass and retention time pairs with the associated intensities for all the peak detected. The parameters of the processing method were as follows: mass window (0.05 Da), RT window (0.2 min), mass tolerance (10 mDa), high and low mass (1000 and 50, respectively), and initial and final retention times (0 and 16 min, respectively).

3. Results

3.1 Body weight gain (BWG)

The BWG of the rats increased in the first eight weeks and decreased after the eighth week (Fig. 1). Compared with that of the control group, the BWG in different treated groups showed no significant changes at each time point ($P > 0.05$). Therefore, BWG is not a sensitive index of acephate-induced toxicity.

3.2 Histopathology

Minor vacuolar degeneration of the liver cytosol and fatty degeneration were observed in the middle-dose group 12 weeks after treatment. Histopathological changes were more evident in the high-dose group than in the middle-dose group 12 weeks after treatment. Furthermore, liver cell cytoplasm vacuolar degeneration, fat degeneration, and liver cell necrosis were exacerbated. No significant histopathological changes were found in the liver tissues of the rats in the low-dose group and the control group (Fig. 2).

3.3 Biochemical indices

The biochemical indices in the serum were determined to monitor the toxic effects of acephate in the 24th week. No significant changes were observed in the low-dose group compared with the control group ($P > 0.05$). Exposure to acephate resulted in a significant increase in LDL, TG, TCHO, and FFA contents (Table 1). Furthermore, HDL contents (Table 1) significantly decreased in middle- and high-dose groups compared with those of the control group ($P < 0.05$ or $P < 0.01$). SOD activity (Fig. 3) significantly decreased whereas MDA levels (Fig. 4) and PLA2 activity (Fig. 5) significantly increased in middle- and high-dose groups compared with those in the control group ($P < 0.05$ or $P < 0.01$).

3.4 Metabolic profiling

Plasma samples from the control group and the treated groups were analyzed using UPLC/ESI-Q-TOF/MS in both positive and negative ionization modes. Representative base peak intensity (BPI) chromatograms of plasma in negative mode in control and high-dose group at week 24 and a typical mass spectra in the negative mode are shown in Fig. 6. Supervised partial least squares discriminant analysis (PLS-DA) models were constructed based on the four groups to understand the metabolic changes and characterize the metabolite profile of the control samples and the treated samples. The representative plot of the PLS-DA scores of the plasma in the positive mode is shown in Fig. 7. In Fig. 7A (four weeks after treatment), the data points did not separate from one another. In Fig. 7B (eight weeks after treatment), the data points of the high-, middle-, and low-dose groups were separated from those of the control group, but overlaps were observed among the treated groups. In Fig. 7C (12 weeks after treatment), the data points of the treated groups were separated from those of the control group, particularly in the high-dose group, but overlaps were evident between low- and middle-dose groups. In Fig. 7E (20 weeks after treatment), the data points of the treated groups were separated from those of the control group, but overlaps were observed between high- and middle-dose groups. In Fig. 7F (24 weeks after treatment), the data points of the treatment groups were clearly separated from those of the control group, and the clusters of each group were very close.

To identify biomarkers, we arranged the analyzed ions in descending order according to VIP values; variables with VIP values >1.0 and those that were dominant

in the loading plots were initially selected. A total of ten metabolites (seven from the positive mode and three from the negative mode) were preliminarily identified. Their *m*/*z* and retention time, postulated identity, and elemental composition are shown in Table 2. Seven metabolites were observed in a representative loading plot of the positive mode on the 12th week (Fig. 8). The changes in ions in both positive and negative modes are presented in Table 3. The results revealed statistically significant changes in some of the metabolites in the treated groups compared with those in the control group (Table 3). In the positive mode, lysoPC (15:0), lysoPC (16:0), lysoPC (O-18:0), lysoPC (18:1(9Z)), lysoPC (18:0), and lysoPC (20:4(5Z, 8Z, 11Z, 14Z)) were increased; by contrast, indoleacrylic acid was decreased in the treated group. In the negative mode, tryptophan was decreased; by comparison, arachidonic acid and 12-hydroxyeicosatetraenoic acid (12-HETE) were increased in the treated group. It is a worthy concern that some metabolites in the low-dose group also showed significant changes compared with those in the control group. LysoPC (15:0) and lysoPC (18:1(9Z)) were significantly increased after the rats were treated for 12 weeks ($P < 0.05$ or $P < 0.01$). Tryptophan was decreased significantly on the 24th week ($P < 0.05$).

4. Discussion

No significant changes were observed in the BWG in the three acephate-treated groups at any time point compared with the time-matched control group ($P > 0.05$). Therefore, the BWG of the rats were not sensitive to the toxicity induced by acephate.

In this study, UPLC/Q-TOF/MS-based metabonomics analysis was performed to

detect candidate endogenous metabolites in rat plasma samples treated with acephate. The differences in the metabolic profiles between treated and control groups were detected in the mean PLS-DA plot pattern, which is a supervised pattern recognition technique. Fig. 7 shows the results of the PLS-DA model of plasma in positive mode from treated and control groups. On the 4th week after treatment, the data points did not separate from one another. This result indicated that the treated group and the control group exhibited similar metabolic profiles. On the 8th week after treatment, the data points of the treated groups were separated from those of the control group, but overlaps were observed among the treated groups. This result suggested that the metabolic profiles in the treated groups were different from those in the control group, and acephate elicited toxicity. On the 12th week after treatment, the data points of the high-dose group were clearly separated from those of low- and middle-dose groups. On the 24th week after treatment, the data points of each group were clearly separated from one another, and the clusters of each group were close. These results suggested that the toxic effects of acephate exposure were dose- and time-dependent.

Ten metabolites in rat plasma were identified using UPLC/Q-TOF/MS in positive and negative modes. Table 3 shows the statistical changes in these metabolites at different time points in the treated groups compared with the time-matched control group. These results indicated that these metabolites were considered as the potential biomarkers of acephate-induced toxicity. The biological relationships between these potential biomarkers and the toxic effects induced by acephate were discussed according to the four pathways shown in Fig. 9.

The first pathway is related to the nervous system and amino acid metabolism (Fig. 9). OP pesticides could inhibit acetylcholinesterase (AChE) activity and elicit neurotoxicity. OP pesticides could also induce neurotoxicity via toxic pathways except acetylcholinesterase inhibition. Tryptophan is an essential amino acid, and indoleacrylic acid is one of its metabolites. Previous studies indicated that tryptophan-metabolism disorder is one of the causes of neurodegenerative disorders and hepatic encephalopathy.[24, 25] In the present study, tryptophan and indoleacrylic acid in rat plasma were significantly decreased, suggesting that exposure to acephate caused tryptophan metabolism disorder and affected the nervous system of rats. Our previously published article showed that AChE activities are decreased in middle- and high-dose groups and significantly differ from those in the control group eight weeks after treatment.[7] This result provided further evidence on neurotoxicity induced by acephate in the present study. As shown in Fig. 9, tryptophan and its metabolite indoleacrylic acid not only affected the rat nervous system but also participated in amino acid metabolism. Studies have reported that OP exposure can disrupt tryptophan metabolism in the liver.[26, 27] In the current study, tryptophan and indoleacrylic acid significantly decreased in the plasma, indicating that exposure to acephate could disturb amino acid metabolism, and this result is in accordance with the observation of Gomes *et al*.[28]

The second pathway is related to oxidative stress (Fig. 9). Lysophosphatidylcholines (lysoPC) included lysoPC (15:0), lysoPC (16:0), lysoPC (O-18:0), lysoPC (18:1(9Z)), lysoPC (18:0), and lysoPC (20:4(5Z, 8Z, 11Z, 14Z

LysoPC is one of numerous lipid products formed during the oxidation of LDL.[29] LDL can be oxidized by various factors, including free radicals.[30] Previous studies indicated that exposure to acephate can generate free radicals;[14, 31] intracellular reactive oxygen species (ROS) are then generated after lysoPC-induced membrane destabilization occurs, and this lysoPC-specific oxidant stress enhances cell injury.[32] In the current study, the increase in lysoPC in plasma exposed to acephate indicated that acephate could induce oxidative stress. SOD is one of the antioxidant enzymes, which catalyze the conversion of superoxide radicals to hydrogen peroxide. SOD plays an important role in the prevention of ROS-induced oxidative damage. MDA is one of the major oxidation products of peroxidized polyunsaturated fatty acids, and an increase in MDA formation may be due to an increase in ROS generated by pesticides. In the present study, SOD activity (Fig. 3) was significantly decreased in middle- and high-dose groups compared with that in the control group; by contrast, MDA content (Fig. 4) in the rat serum was significantly increased. These results provided additional support to previously obtained metabonomics results.

The third pathway is involved in lipid metabolism (Fig. 9). Phospholipids are components of cell membranes, and phosphatidylcholine is a kind of membrane phospholipids. Phospholipase A2 (PLA2) catalyzes the hydrolysis of the sn-2 position of membrane glycerophospholipids to generate lysoPC and FFA.[33] Exogenous lysoPC may be delivered to cells and disrupt membranes after the ability of lysoPC to metabolize is exceeded.[32] FFA is a kind of lipid, some studies have indicated that elevated FFA levels can generate ROS.[34] In the current study, lysoPC and FFA

significantly increased in middle- and high-dose groups compared with those of the control group. We presume that the activity of PLA2 in rat serum may be activated by ROS, as induced by acephate. As such, the activity of PLA2 in the serum on the 24th week was determined to prove this presumption. As shown in Fig. 5, the activity of PLA2 was significantly increased in middle- and high-dose groups compared with those of the control group; this result confirmed our presumption. Arachidonic acid is a kind of polyunsaturated fatty acid, and 12-HETE is a metabolite of arachidonic acid. Studies have indicated that OP impairs enzymatic pathways involved in fat metabolism,[35] and this impairment may be accounted for the increase in arachidonic acid and 12-HETE in plasma. In the current study, significant changes in lysoPC, arachidonic acid, and 12-HETE in the rat plasma indicated that exposure to acephate could affect the lipid metabolism of rats. In addition, routine lipid parameters (HDL, LDL, TG, TCHO, and FFA; Table 1) in the rat serum significantly changed in middle- and high-dose groups compared with those in the control group; these results further supported the aforementioned metabonomic results.

The fourth pathway is related to liver function (Fig. 9). As shown in Fig. 9, the metabolites identified in the current study were involved in liver function. Liver is a vital organ and plays a key role in metabolism and detoxification. Hepatic disorder is substantially reported to possibly disturb the balance of endogenous compounds, such as amino acids [36] and fatty acids.[37] Tryptophan is an essential amino acid and can be considered as a potential biomarker of chemical-induced liver injury.[36] Arachidonic acid is a precursor of eicosanoids, including prostaglandins and thromboxanes;

arachidonic acid also plays key roles in many physiological and pathological functions.[38] 12-HETE is an eicosanoid, a 5-lipoxygenase metabolite of arachidonic acid; 12-HETE is also associated with liver injury caused by lipid peroxidation.[39] LysoPC is a natural product resulting from PLA2 activity to remove fatty acids from membrane and lipoprotein phospholipids, and some of lysoPC [such as lysoPC (18:0) and lysoPC (O-18:0)] are used as biomarkers of the degree of liver cell death.[40] Thus, the changes in tryptophan, indoleacrylic acid, arachidonic acid, 12-HETE, and lysoPC in the current study indicated that exposure to acephate could affect liver function. The histopathological changes in the liver (Fig. 2) also supported the aforementioned liver damage.

The histopathological examination results of the liver (Fig. 2) of the rats in the low-dose group did not show any change; by contrast, lysoPC (15:0), lysoPC (18:1(9Z)), and tryptophan in rat plasma significantly increased or decreased using the metabonomics-based method. These results indicated that the NOAEL of acephate obtained using traditional toxicological methods could induce significant changes in the metabolites at body metabolic level. This finding suggested that the aforementioned factor should be considered for the revision of the acceptable daily intake (ADI) of acephate in the future.

In this study, the metabolic profiles of rats chronically exposed to low-level acephate were investigated. As shown in Fig. 9, some metabolites in rat plasma were significantly altered which indicated that these metabolites could served as the potential biomarkers of the toxicity induced by acephate. These significantly altered

metabolites indicated that exposure to acephate could disrupt metabolism (such as lipid and amino acid metabolism) and induce oxidative stress, neurotoxicity, and liver dysfunction. Our previously published article investigated the toxic effects of acephate in the urine of rats by metabonomic technology, indicating that exposure to acephate could lead to rat renal injury and abnormal metabolism of substances, including glucose, nucleic acid, and protein metabolism.[7] The results in the present study provide further support and complementaries for the aforementioned article. The combination of plasma and urine metabonomic analyses is conducive for the systematic understanding of the toxic effects of acephate. The analysis of metabolic profiles in plasma samples treated with acephate could also provide a reference for human chronic exposure to low-level acephate.

Conflict of interest

The authors declared that they have no conflicts of interest in this work.

Acknowledgements

Financial support from the National Natural Scinence Foundation of China (30972490) is gratefully acknowledged.

References

1 S. Mohapatra, A. K. Ahuja, M. Deepa and D. Sharma, *Bulletin of environmental contamination and toxicology*, 2011, 86, 101-104.
2 M.A.Hussain, *Bulletin of environmental contamination and toxicology*, 1987, 38, 131-138.
3 G. F. Antonious and J. C. Snyder, *Bulletin of environmental contamination and toxicology*, 1994, 52, 141-148.

4 G.B.Jena and S.P.Bhunya, *Mutagenesls*, 1994, 9, 319-324.

5 T. Chuanjiang, L. Dahui, Z. Xinzhong, C. Shanshan, F. Lijuan, P. Xiuying, S. Jie, J. Hui, L. Chongjiu and L. Jianzhong, *Environmental monitoring and assessment*, 2010, 165, 685-692.

6 Z. Feng and J. Li, *Journal of Traditional Chinese Veterinary Medicine*, 2003, 21, 40-42.

7 D.-F. Hao, W. Xu, H. Wang, L.-F. Du, J.-D. Yang, X.-J. Zhao and C.-H. Sun, *Ecotoxicology and environmental safety*, 2012, 83, 25-33.

8 V. Dhull, A. Gahlaut, N. Dilbaghi and V. Hooda, *Biochemistry research international*, 2013, 2013, 731501.

9 http://www.inchem.org.

10 A. Sapone, L. Pozzetti, D. Canistro, M. Broccoli, G. Bronzetti, G. Potenza, A. Affatato, G. L. Biagi, G. Cantelli-Forti and M. Paolini, *Food and chemical toxicology : an international journal published for the British Industrial Biological Research Association*, 2005, 43, 173-183.

11 M.F.Rahman, M.Mahboob, K.Danadevi, B. S. Banu and P. Grover, *Mutation Research*, 2002, 516, 139-147.

12 D. Ozkan, D. Yuzbasioglu, F. Unal, S. Yilmaz and H. Aksoy, *Cytotechnology*, 2009, 59, 73-80.

13 A. Thapar, R. Sandhir and R. Kiran, *Indian Journal of Experimental Biology*, 2002, 40, 963-966.

14 S. Datta, P. Dhar, A. Mukherjee and S. Ghosh, *Food and chemical toxicology : an international journal published for the British Industrial Biological Research Association*, 2010, 48, 2766-2771.

15 J. Yang, J. Cao, X. Sun, Z. Feng, D. Hao, X. Zhao and C. Sun, *Cell biochemistry and function*, 2012, 30, 122-128.

16 J. K. Nicholson, J. C. Lindon and E. Holmes, *Xenobiotica*, 1999, 29, 1181-1189.

17 M. Bogdanov, W. R. Matson, L. Wang, T. Matson, R. Saunders-Pullman, S. S. Bressman and M. Flint Beal, *Brain : a journal of neurology*, 2008, 131, 389-396.

18 D. G. Robertson, *Toxicological sciences : an official journal of the Society of Toxicology*, 2005, 85, 809-822.

19 A. Roux, D. Lison, C. Junot and J. F. Heilier, *Clinical biochemistry*, 2011, 44, 119-135.

20 I. Dudka, B. Kossowska, H. Senhadri, R. Latajka, J. Hajek, R. Andrzejak, J. Antonowicz-Juchniewicz and R. Gancarz, *Environment international*, 2014, 68, 71-81.

21 C. Chen, K. W. Krausz, Y. M. Shah, J. R. Idle and F. J. Gonzalez, *Chemical research in toxicology*, 2009, 22, 699-707.

22 L. Wei, P. Liao, H. Wu, X. Li, F. Pei, W. Li and Y. Wu, *Toxicology and applied pharmacology*, 2009, 234, 314-325.

23 L. Du, S. Li, L. Qi, Y. Hou, Y. Zeng, W. Xu, H. Wang, X. Zhao and C. Sun, *Molecular bioSystems*, 2014, 10, 1153-1161.

24 K. Schrocksnadel, B. Wirleitner, C. Winkler and D. Fuchs, *Clinica chimica acta; international journal of clinical chemistry*, 2006, 364, 82-90.

25 T. W. Stone, C. M. Forrest, G. M. Mackay, N. Stoy and L. G. Darlington, *Metabolic brain disease*, 2007, 22, 337-352.
26 T. Pewnim and J. Seifert, *European Journal of Pharmacology-Environmental Toxicology and Pharmacology*, 1993, 248, 237-241.
27 R. Rahimi and M. Abdollahi, *Pesticide Biochemistry and Physiology*, 2007, 88, 115-121.
28 J. Gomes, A. Dawodu, O. Lloyd, D. Revitt and S. Anilal, *Human & experimental toxicology*, 1999, 18, 33-37.
29 B. K. Yoon, Y. H. Kang, W. J. Oh, K. Park, D. Y. Lee, D. Choi, D. K. Kim, Y. Lee and M. R. Rhyu, *Journal of Korean medical science*, 2012, 27, 803-810.
30 A. Mertens and P. Holvoet, *FASEB Journal*, 2001, 15, 2073-2084.
31 V. S. Poovala, V. K. Kanji, H. Tachikawa and A. K. Salahudeen, *Toxicological Sciences*, 1998, 46, 403-409.
32 S. M. Colles and G. M. Chisolm, *Journal of lipid research*, 2000, 41, 1188-1198.
33 M. Murakami, Y. Taketomi, Y. Miki, H. Sato, T. Hirabayashi and K. Yamamoto, *Progress in lipid research*, 2011, 50, 152-192.
34 J. L.Evans, I. D.Goldfine, B. A.Maddux and G. M.Grodsky, *Diabetes*, 2003, 54, 1-8.
35 S. Karami-Mohajeri and M. Abdollahi, *Human & experimental toxicology*, 2011, 30, 1119-1140.
36 Y. Xu, L. Yang, F. Yang, Y. Xiong, Z. Wang and Z. Hu, *Metabolomics*, 2011, 8, 475-483.
37 A. Berlanga, E. Guiu-Jurado, J. A. Porras and T. Auguet, *Clinical and experimental gastroenterology*, 2014, 7, 221-239.
38 H. Nakamura and T. Murayama, *Journal of Pharmacological Sciences*, 2014, 124, 307-312.
39 M. Morita, N. Ishida, K. Uchiyama, K. Yamaguchi, Y. Itoh, M. Shichiri, Y. Yoshida, Y. Hagihara, Y. Naito, T. Yoshikawa and E. Niki, *Free radical research*, 2012, 46, 758-765.
40 E. Gonzalez, S. van Liempd, J. Conde-Vancells, V. Gutierrez-de Juan, M. Perez-Cormenzana, R. Mayo, A. Berisa, C. Alonso, C. A. Marquez, J. Barr, S. C. Lu, J. M. Mato and J. M. Falcon-Perez, *Metabolomics*, 2012, 8, 997-1011.

Figure Captions

Fig. 1 The body weight gain (BWG) of rats exposed to acephate at each time and dose. Each bar represents means ± SD (n=5). C, control group; L, low-dose group; M, middle-dose group; H, high-dose group.

Fig. 2 The photomicrographs of liver 12 weeks after treatment. (A) control group, (B) low-dose group, (C) middle-dose group, (D) high-dose group. HE stain, magnification, 200×.

Fig. 3 The activity of SOD in rat serum 24 weeks after treatment. C, control group; L, low-dose group; M, middle-dose group; H, high-dose group. Each bar represents means ± SD (n=5). * Significantly different from control rats at $P < 0.05$, ** Significantly different from control rats at $P < 0.01$ (one-way ANOVA).

Fig. 4 The contents of MDA in rat serum 24 weeks after treatment. C, control group; L, low-dose group; M, middle-dose group; H, high-dose group. Each bar represents means ± SD (n=5). * Significantly different from control rats at $P < 0.05$, ** Significantly different from control rats at $P < 0.01$ (one-way ANOVA).

Fig. 5 The activity of PLA2 in rat serum 24 weeks after treatment. C, control group; L, low-dose group; M, middle-dose group; H, high-dose group. Each bar represents means ± SD (n=5). ** Significantly different from control rats at $P < 0.01$ (one-way

ANOVA).

Fig. 6 The representative BPI chromatograms of plasma in negative mode in control and high-dose group at week 24 and a typical mass spectrum. (A) the BPI chromatograms of control group. (B) the BPI chromatograms of high-dose group. (C) the typical mass spectra of arachidonic acid in negative mode.

Fig. 7 PLS-DA score plots of plasma in the positive mode. PLS-DA score t[1] versus t[2] of data obtained from mean variables of plasma collected from the control and treated groups. ■,control group; ●, low-dose group; ▲, middle-dose group; ◆, high-dose group. (A-F), 0, 4, 8, 12, 16, 20, 24 weeks after treatment.

Fig. 8 Loading plot based on the plasma profiling in the positive mode 12 weeks after treatment.

Fig. 9 The disturbed metabolism pathways in response to acephate exposure. ↑ The intensity of the metabolite was significantly increased in the treated groups compared with the control group; ↓ The intensity of the metabolite was significantly decreased in the treated groups compared with the control group group.

Table 1 Effect of acephate on serum routine lipid parameters and FFA level

Groups (n=5)	HDL(mmol/L)	LDL(mmol/L)	TG(mmol/L)	TCHO(mmol/L)	FFA(μmol/L)
C	0.94±0.13	0.34±0.06	0.72±0.07	1.86±0.16	1053.05±100.25
L	0.88±0.06	0.38±0.07	0.92±0.18	2.07±0.18	1123.29±136.02
M	0.75±0.13*	0.50±0.05**	1.02±0.10**	2.26±0.27*	1383.74±139.99**
H	0.71±0.08**	0.58±0.10**	1.36±0.12**	2.49±0.12**	1539.20±153.29**

Note: C, control group; L, low-dose group; M, middle-dose group; H, high-dose group.
* Significantly different from control rats at $P < 0.05$ (one-way ANOVA).
** Significantly different from control rats at $P < 0.01$ (one-way ANOVA).

Table 2 Potential biomarkers of toxicity induced by acephate

Retention time (min)	Measured *m/z* ion (Da)	Calculated *m/z* ion (Da)	Error of *m/z* (Da)	Error of *m/z* ppm	Elemental composition	Scan mode	Metabolites
2.61	188.0728	188.0700	0.0028	14.8	$C_{11}H_9NO_2$	+	Indoleacrylic acid
7.17	482.3240	482.3241	0.0001	0.21	$C_{23}H_{48}NO_7P$	+	LysoPC(15:0)
7.73	496.3351	496.3397	0.0046	9.2	$C_{24}H_{50}NO_7P$	+	LysoPC(16:0)
8.29	510.3950	510.3918	0.0032	6.2	$C_{26}H_{56}NO_6P$	+	LysoPC(O-18:0)
7.96	522.3520	522.3554	0.0034	6.5	$C_{26}H_{52}NO_7P$	+	LysoPC(18:1(9Z))
8.97	524.3658	524.3710	0.0052	9.9	$C_{26}H_{54}NO_7P$	+	LysoPC(18:0)
7.33	544.3387	544.3397	0.0010	1.8	$C_{28}H_{50}NO_7P$	+	LysoPC(20:4(5Z,8Z,11Z,14Z))
2.54	203.0803	203.0820	0.0017	8	$C_{11}H_{12}N_2O_2$	-	Tryptophan
9.28	303.2279	303.2330	0.0051	16.8	$C_{20}H_{32}O_2$	-	Arachidonic acid
5.46	319.2236	319.2279	0.0043	13	$C_{20}H_{32}O_3$	-	12-HETE

Table 3 Summary of intensity values of biomarkers detected in positive ESI mode and negative ESI mode in rats' plasma

Peak intensity (mean±SD, n=5)											
Times (Week)		Positive mode							Negative mode		
	Groups	Indoleacrylic acid	LysoPC(15:0)	LysoPC(16:0)	LysoPC(O-18:0)	LysoPC(18:1(9Z))	LysoPC(18:0)	LysoPC(20:4(5Z,8Z,11Z,14Z))	Tryptophan	Arachidonic acid	12-HETE
4	C	131.9±14.1	17.8±1.7	348.5±27.3	2.8±0.7	21.7±2.7	117.9±10.2	265.8±34.3	118.8±10.3	202.4±34.8	21.3±7.8
	L	124.5±12.4	19.3±3.9	381.7±47.8	3.0±0.3	23.4±2.3	119.3±10.5	280.5±28.8	116.4±17.9	208.6±24.3	19.4±2.7
	M	126.6±13.1	22.4±2.6*	365.1±25.8	2.9±0.3	26.3±2.2*	114.7±14.6	300.1±17.4	98.5±13.2*	240.5±45.2	24.5±7.9
	H	110.4±12.6*	22.4±2.3*	403.6±36.8*	3.5±0.3*	26.6±2.4*	140.6±15.9*	313.1±28.6*	95.5±10.2*	260.1±26.6*	31.8±4.7*
8	C	135.6±16.5	17.0±2.0	332.3±41.5	3.0±0.2	22.9±3.9	111.9±9.8	219.9±33.6	115.3±8.0	202.2±31.3	16.9±6.4
	L	125.8±11.9	19.9±1.6	321.7±20.0	3.1±0.3	24.3±3.9	112.8±11.0	236.9±12.5	122.5±19.4	217.5±20.5	23.6±5.0
	M	120.8±15.1	21.2±3.1*	383.8±31.2*	3.4±0.3*	29.5±3.3*	130.6±11.9*	271.5±27.2*	93.0±11.9*	255.0±35.0*	27.5±4.1*
	H	108.7±14.5*	21.0±3.0*	404.5±23.6**	3.6±0.2**	29.6±4.7*	134.4±12.2**	292.8±34.6**	90.5±15.3*	282.9±50.7**	29.9±8.3**
12	C	132.8±11.6	16.2±1.6	330.4±68.5	3.6±0.4	23.2±4.5	109.3±11.4	272.5±30.7	134.1±11.8	231.5±60.6	26.4±5.2
	L	124.9±9.2	22.5±2.6*	354.6±22.6	4.0±0.2	34.8±7.9*	116.2±11.4	282.6±13.0	127.1±15.4	265.6±25.1	28.2±7.0
	M	112.9±14.3*	23.3±3.5**	415.6±47.5*	4.2±0.5*	36.2±6.3**	134.5±15.1*	340.0±25.9**	81.6±11.1**	313.3±62.6*	37.9±8.2*
	H	108.1±12.4**	27.1±5.6**	447.3±36.4**	4.5±0.3**	38.1±7.9**	145.3±16.4**	356.5±30.5**	88.8±11.6**	333.2±56.2**	40.8±5.6**
16	C	128.3±9.8	16.1±1.9	327.6±43.3	3.8±0.4	24.1±7.3	111.4±13.0	280.3±19.9	149.4±19.8	212.6±27.9	23.8±7.6
	L	117.4±14.5	20.8±2.3*	380.6±34.1	3.9±0.3	38.6±7.3*	118.0±16.8	257.1±29.1	139.8±12.4	219.4±35.8	29.7±3.2
	M	103.0±11.8**	22.9±3.8**	440.2±62.7**	4.9±0.3**	42.7±9.8**	149.7±15.2**	357.8±22.8**	108.4±12.9**	292.5±61.6**	35.9±3.0**
	H	99.7±12.3**	25.6±2.5**	472.9±48.1**	5.2±0.3**	44.6±9.1**	152.9±22.8**	374.2±48.8**	100.9±10.5**	316.7±27.6**	42.7±7.7**
20	C	133.5±11.9	19.2±2.9	328.7±40.3	3.8±0.5	24.7±3.7	106.4±13.0	274.5±42.4	124.5±20.5	172.1±31.9	22.3±8.1
	L	117.5±12.7	23.9±2.0*	393.1±27.4	4.1±0.3	41.5±8.2**	112.0±18.1	321.7±31.7	109.1±9.9	207.1±30.7	23.4±6.6
	M	101.9±8.0**	26.0±2.5**	450.9±54.9**	5.1±0.2**	43.5±6.8**	145.7±13.4**	370.3±58.9**	93.3±12.3**	272.6±47.3**	33.9±3.2**
	H	97.3±15.8**	28.6±3.8**	478.4±53.9**	5.4±0.5**	44.2±9.6**	150.9±20.5**	408.3±19.5**	87.6±10.9**	298.0±33.0**	39.3±5.0**
24	C	124.0±13.2	17.4±2.8	318.6±19.5	4.1±0.5	26.7±3.7	112.5±14.4	234.7±17.7	122.6±13.2	209.5±44.1	21.8±3.3
	L	113.9±11.5	24.8±4.7**	376.1±43.9	4.3±0.7	43.5±8.2**	120.2±13.6	273.8±44.6	101.1±13.2*	265.6±25.1	21.3±3.4
	M	99.7±8.84**	25.6±2.2**	447.2±44.9**	5.5±0.5**	45.7±6.9**	148.7±20.8**	356.4±38.5**	85.7±16.8**	295.3±51.8**	32.1±3.5**
	H	94.1±9.6**	27.5±2.6**	486.3±65.7**	5.8±0.3**	47.2±9.6**	154.5±16.6**	388.3±40.1**	89.3±8.9**	335.2±53.9**	39.4±5.7**

Note: C, control group; L, low-dose group; M, middle-dose group; H, high-dose group.

* Significantly different from control rats at $P < 0.05$ (ANCOVA)

**Significantly different from control rats at $P < 0.01$ (ANCOVA).

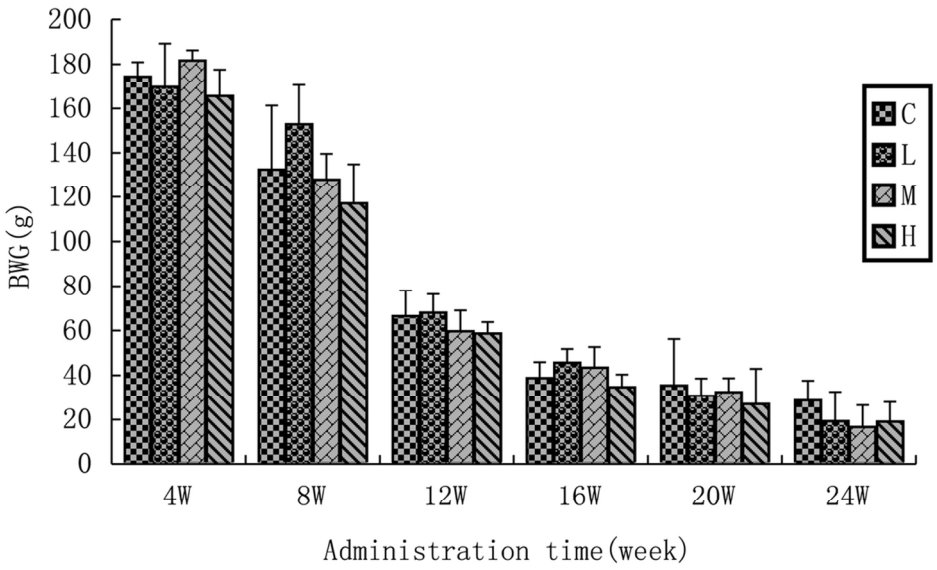

Fig. 1 The body weight gain (BWG) of rats exposed to acephate at each time and dose. Each bar represents means±SD (n=5). C, control group; L, low-dose group; M, middle-dose group; H, high-dose group.
107x67mm (300 x 300 DPI)

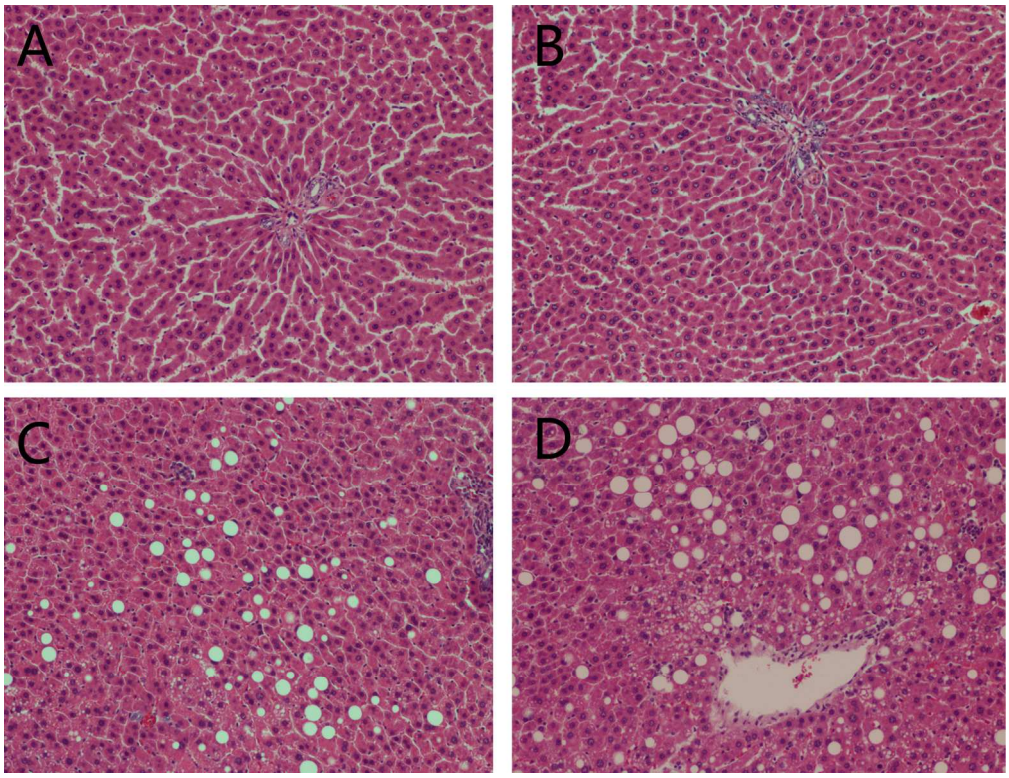

Fig. 2 The photomicrographs of liver 12 weeks after treatment. (A) control group, (B) low-dose group, (C) middle-dose group, (D) high-dose group. HE stain, magnification, 200×
157x120mm (300 x 300 DPI)

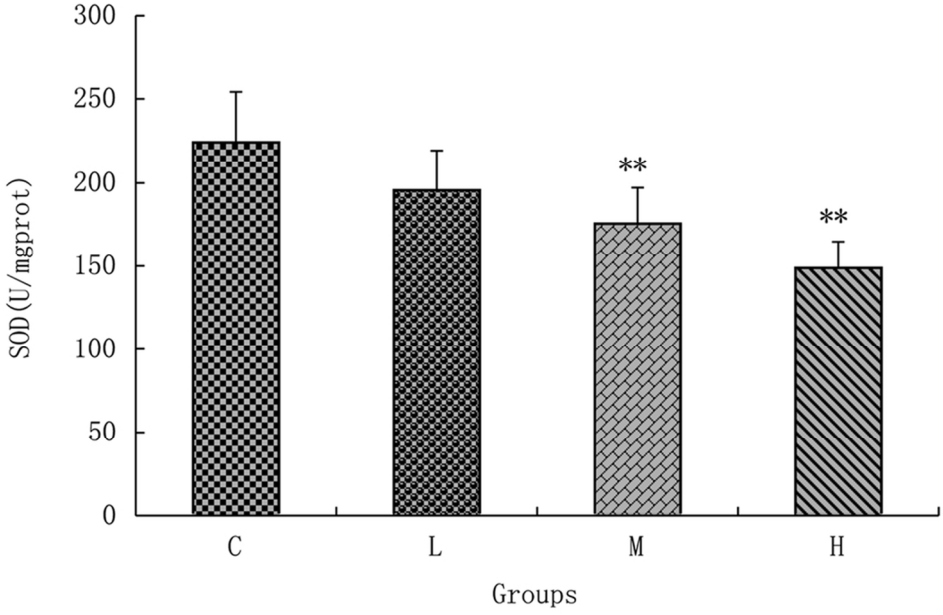

Fig. 3 The activity of SOD in rat serum 24 weeks after treatment. C, control group; L, low-dose group; M, middle-dose group; H, high-dose group. Each bar represents means±SD (n=5). * Significantly different from control rats at $P < 0.05$, ** Significantly different from control rats at $P < 0.01$ (one-way ANOVA).
93x60mm (300 x 300 DPI)

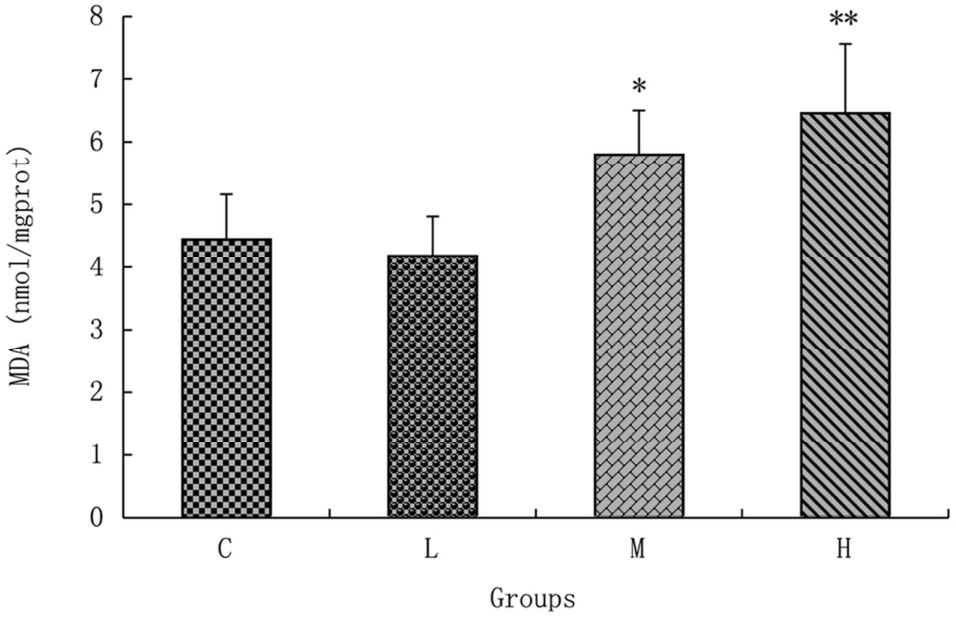

Fig. 4 The contents of MDA in rat serum 24 weeks after treatment. C, control group; L, low-dose group; M, middle-dose group; H, high-dose group. Each bar represents means±SD (n=5). * Significantly different from control rats at $P < 0.05$, ** Significantly different from control rats at $P < 0.01$ (one-way ANOVA).
94x61mm (300 x 300 DPI)

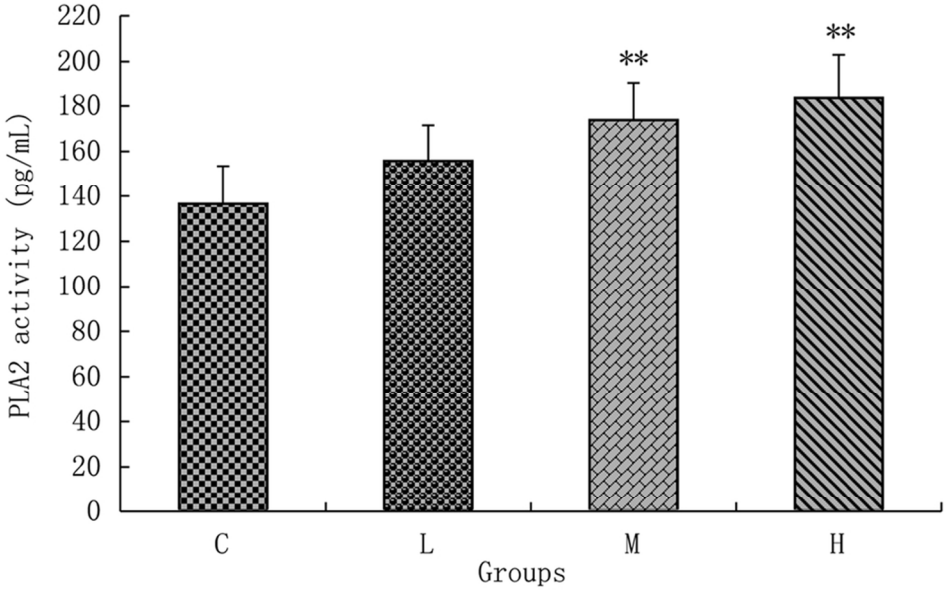

Fig. 5 The activity of PLA2 in rat serum 24 weeks after treatment. C, control group; L, low-dose group; M, middle-dose group; H, high-dose group. Each bar represents means±SD (n=5). ** Significantly different from control rats at $P < 0.01$ (one-way ANOVA).
90x56mm (300 x 300 DPI)

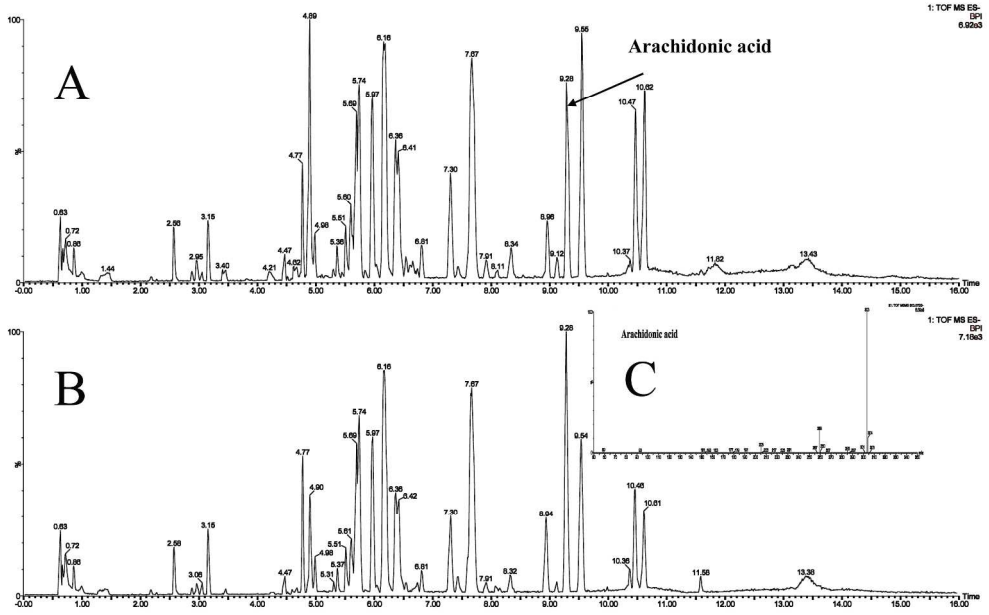

Fig. 6 The representative BPI chromatograms of plasma in negative mode in control and high-dose group at week 24 and a typical mass spectrum. (A) the BPI chromatograms of control group. (B) the BPI chromatograms of high-dose group. (C) the typical mass spectra of arachidonic acid in negative mode.
251x157mm (300 x 300 DPI)

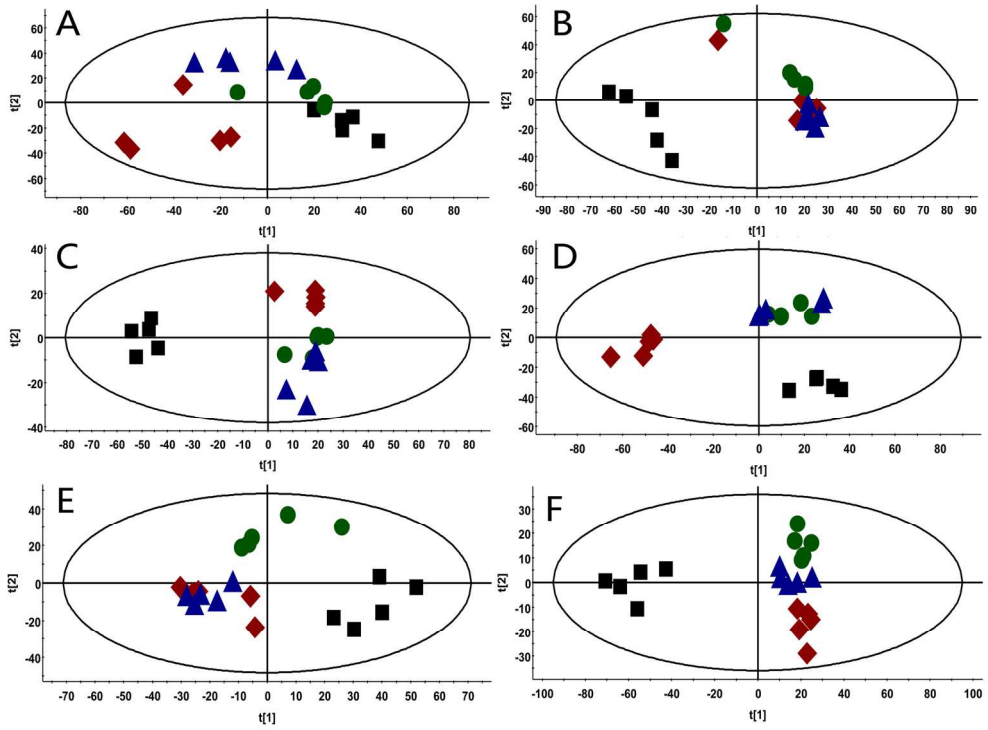

Fig. 7 PLS-DA score plots of plasma in the positive mode. PLS-DA score t[1] versus t[2] of data obtained from mean variables of plasma collected from the control and treated groups. ■,control group; ●, low-dose group; ▲, middle-dose group; ◆, high-dose group. (A-F), 0, 4, 8, 12, 16, 20, 24 weeks after treatment.
159x118mm (300 x 300 DPI)

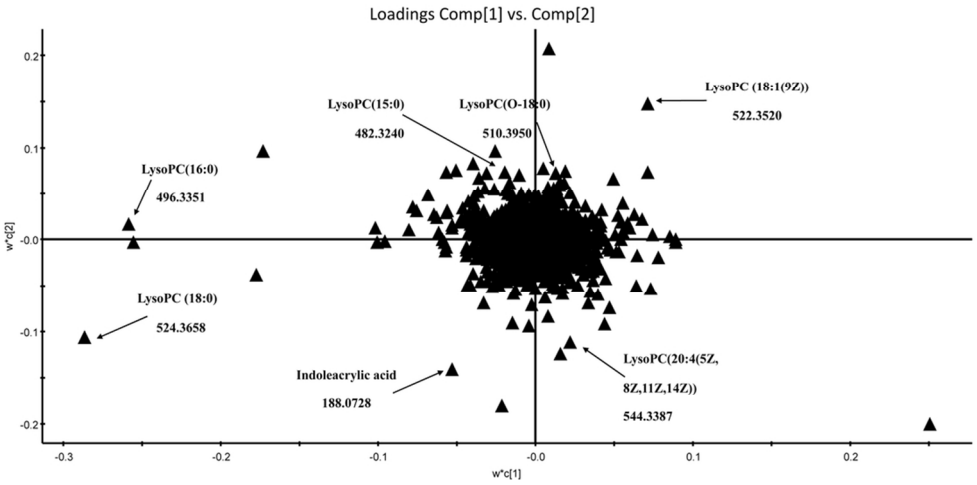

Fig. 8 Loading plot based on the plasma profiling in the positive mode 12 weeks after treatment.
96x49mm (300 x 300 DPI)

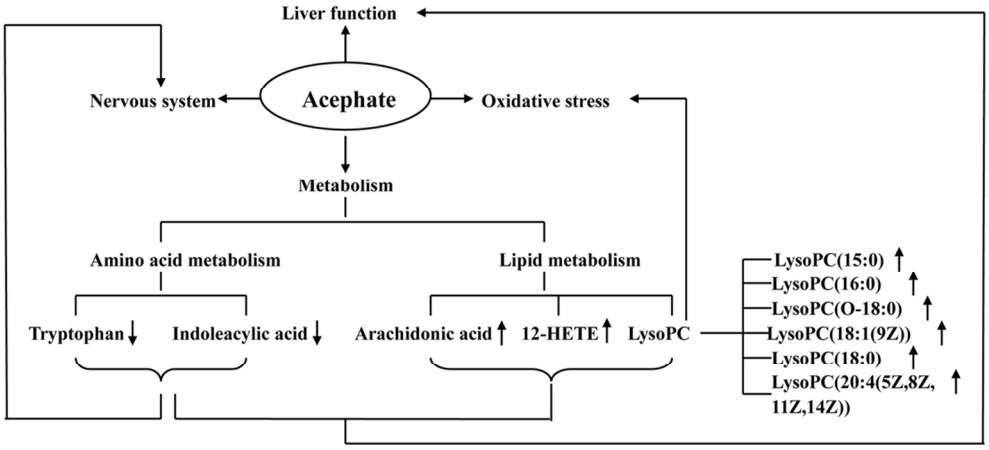

Fig. 9 The disturbed metabolism pathways in response to acephate exposure. ↑ The intensity of the metabolite was significantly increased in the treated groups compared with the control group; ↓ The intensity of the metabolite was significantly decreased in the treated groups compared with the control group group.
102x46mm (300 x 300 DPI)